

## Strand Invasion of Mixed-Sequence B-DNA by Acridine-Linked, $\gamma$ -Peptide Nucleic Acid ( $\gamma$ -PNA)

Srinivas Rapireddy, Gaofei He, Subhadeep Roy, Bruce A. Armitage, and Danith H. Ly\*

Contribution from the Department of Chemistry, Carnegie Mellon University, 4400 Fifth Avenue, Pittsburgh, Pennsylvania 15213

Received July 3, 2007; E-mail: dly@andrew.cmu.edu

**Abstract:** Peptide nucleic acid (PNA) is a synthetic mimic of DNA and RNA that can recognize double-stranded B-DNA through direct Watson–Crick base-pairing. Although promising, PNA recognition is presently limited to mostly purine- and pyrimidine-rich targets, because mixed-sequence PNA, in general, does not have sufficient binding free energy to invade B-DNA. In this Article, we show that conformationally preorganized  $\gamma$ -peptide nucleic acid ( $\gamma$ -PNA) containing an acridine moiety covalently linked at the C-terminus can invade mixed-sequence B-DNA in a sequence-specific manner. Recognition occurs through direct Watson–Crick base-pairing. This finding is significant because it demonstrates that the same principles that guide the recognition of single-stranded DNA and RNA can also be applied to double-stranded B-DNA.

### Introduction

Watson–Crick base-pairings, the specific interactions between A–T (or A–U) and G–C nucleobases, are the fundamental principles of nucleic acid recognition, important not only for the storage and transmission of genetic information but also for a variety of biotechnology applications, including antisense.<sup>1</sup> With knowledge of the sequence information, one can design the corresponding oligonucleotides to bind to the targets based on this simple set of rules. However simple, these principles can only be applied to the recognition of single-stranded DNA or RNA. Recognition of double helical B-form DNA (B-DNA), on the other hand, is more difficult to accomplish because the chemical groups responsible for such interactions are no longer available for binding; instead, they form their own base-pairs and are buried deep within the double helix.<sup>2</sup> Gaining access to these functional groups would require base-pair opening, a process thought to be exceedingly slow and energetically inaccessible to most exogenous molecules.<sup>3</sup> However, a recent series of studies by Nielsen and co-workers<sup>4</sup> showed that B-DNA could be targeted sequence-specifically by peptide nucleic acid (PNA), a synthetic mimic of DNA and RNA, through Watson–Crick base-pairing. Although appealing, this recognition strategy is presently limited to mostly purine- and pyrimidine-rich targets, because mixed-sequence PNA, in general, does not have sufficient binding free energy to invade B-DNA. Although a double-duplex invasion strategy has recently been developed to relax this sequence constraint,<sup>5,6</sup> limitations in sequence selection still remain due to the unre-

solved issue with self-quenching. In this Article, we show that conformationally preorganized  $\gamma$ -PNA containing a terminally linked acridine moiety can strand-invade mixed-sequence B-DNA; however, unlike the other invasion strategies developed to date,<sup>5,7,8</sup> only a single strand of  $\gamma$ -PNA is required and no triplex-forming element is necessary. This finding is significant because it demonstrates that the same principles that guide the recognition of single-stranded DNA and RNA can also be applied to double-stranded B-form DNA.

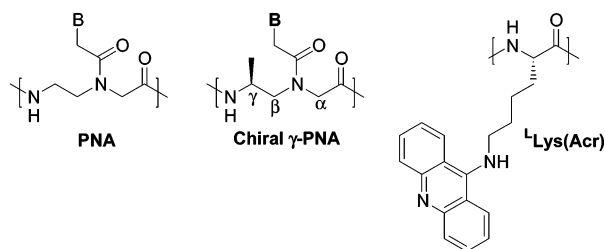
### Results and Discussion

**Rationale.** Because PNA, in general, does not have a well-defined conformation,<sup>9–12</sup> we reasoned that the required binding energetics could be attained if PNA could be preorganized prior to binding to its designated B-DNA target. Conformational preorganization is expected to improve the invasion kinetics, as well as thermodynamics because minimal structural reorganization would be required prior or subsequent to complexation.<sup>13,14</sup> We recently reported the development of this particular class of chiral PNA molecules, whereby we showed that installation of (*R*)-chiral centers at the  $\gamma$ -positions of the *N*-(2-aminoethyl) glycine backbone units transformed randomly

- (1) Mesmaeker, A.; Haner, R.; Martin, P.; Moser, H. E. *Acc. Chem. Res.* **1995**, *28*, 366–374.
- (2) Watson, J. D.; Crick, F. H. C. *Nature* **1953**, *171*, 737–738.
- (3) Frank-Kamenetskii, M. D. *Nature* **1987**, *328*, 17–18.
- (4) Nielsen, P. E. *Acc. Chem. Res.* **1999**, *32*, 624–630 and references therein.
- (5) Lohse, J.; Dahl, O.; Nielsen, P. E. *Proc. Natl. Acad. Sci. U.S.A.* **1999**, *96*, 11804–11808.

- (6) Demidov, V. V.; Protozanova, E.; Izvol'sky, K. I.; Price, C.; Nielsen, P. E.; Frank-Kamenetskii, M. D. *Proc. Natl. Acad. Sci. U.S.A.* **2002**, *99*, 5953–5958.
- (7) Bentin, T.; Larsen, H. J.; Nielsen, P. E. *Biochemistry* **2003**, *42*, 13987–13995.
- (8) Kaihatsu, K.; Shah, R. H.; Zhao, X.; Corey, D. R. *Biochemistry* **2003**, *42*, 13996–14003.
- (9) Gildea, B. D.; Coull, J. M.; Hyldig-Nielsen, J. J.; Fiandaca, M. J. *WO A-9921881*, 1999.
- (10) Tackett, A. J.; Corey, D. R.; Raney, K. D. *Nucleic Acids Res.* **2002**, *30*, 950–957.
- (11) Seitz, O. *Angew. Chem., Int. Ed.* **2000**, *39*, 3249–3252.
- (12) Ranasinghe, R. T.; Brown, L. J.; Brown, T. *Chem. Commun.* **2001**, 1480–1481.
- (13) Cram, D. J. *Science* **1988**, *240*, 760–767.
- (14) Kool, E. T. *Chem. Rev.* **1997**, *97*, 1473–1487.

**Scheme 1.** Chemical Structure of PNA and (*R*)-Alanyl- $\gamma$ -PNA (Bold) Building Blocks, along with the Structure of Acridine-Linked L-Lysine Residue



folded, single-stranded PNA into a right-handed helix.<sup>15</sup> These helical  $\gamma$ -PNAs exhibited unusually strong affinity and sequence-specificity for single-stranded DNA;<sup>15</sup> however, their ability to invade double-stranded B-DNA had not yet been determined. To address this issue, we synthesized three homologous dodecameric PNA oligomers (PNA1, PNA2, and PNA3, Scheme 1). PNA1 contained an unmodified backbone and was used as a negative control. PNA2 differs from PNA1 in that it contained fully modified, (*R*)-alanyl- $\gamma$ -backbone units. PNA3 is identical to PNA2 except that it contained an acridine moiety at the C-terminus, appended to the L-lysine side-chain. Acridine was included because prior studies showed that it can significantly stabilize DNA binding.<sup>16–18</sup> All chiral  $\gamma$ -PNA monomers were prepared following a newly developed method, which yielded high optical purity.<sup>19</sup> PNA and  $\gamma$ -PNA oligomers were synthesized on solid-support under identical conditions in accordance with the established procedures<sup>20</sup> and were purified and characterized by RP-HPLC and MALDI-TOF mass spectrometry, respectively.

**Conformational Preorganization.** To confirm that these  $\gamma$ -PNAs adopted right-handed helical structures, we measured the CD spectra of PNA1–3 in 10 mM sodium phosphate (NaPi) buffer (pH 7.4) and compared them to that of the corresponding PNA–DNA hybrid duplex. Consistent with the previous findings,<sup>15,21</sup> we observed a pronounced biphasic exciton coupling pattern characteristic of a right-handed helix<sup>22</sup> for PNA2 and PNA3, and none for PNA1, in the nucleobase absorption regions (Figure 1A). The CD profiles of PNA2 and PNA3 are similar to that of the corresponding hybrid duplexes shown in Figure 1B. The only difference is in the amplitude, which can be accounted for by the difference in the strand concentration, twice for the duplex as compared to the single strand. We ruled out the possibility of inter- and/or intramolecular self-hybridization

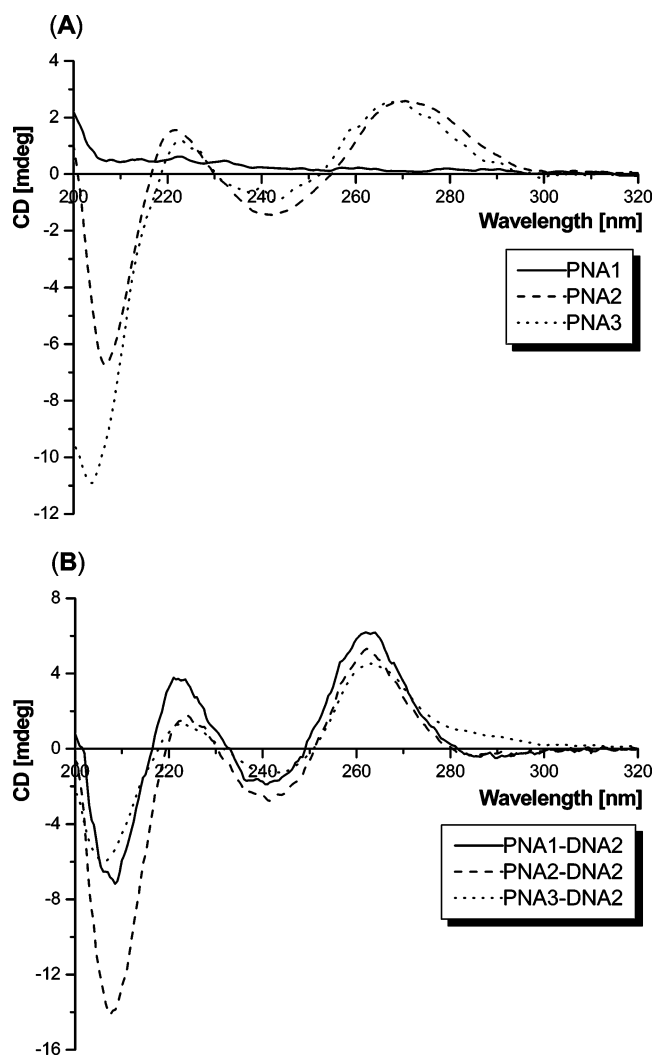


**Figure 1.** (A) CD spectra of single-stranded PNA1, PNA2, and PNA3 at 2  $\mu$ M strand concentration each in 10 mM NaPi buffer (pH 7.4), recorded at room temperature. (B) CD spectra of the corresponding PNA–DNA hybrid duplex at 2  $\mu$ M strand concentration each, recorded at room temperature after annealing in the same buffer. DNA2: 5'-ATCTGTGGTC-3'.

of PNA2 or PNA3 on the basis of <sup>1</sup>H NMR results (unpublished data), which showed that at a concentration as high as 2 mM, no imino proton signals in the 10–14 ppm regions indicative of Watson–Crick H-bonding were observed. The existence of helical structures in single-stranded oligonucleotides is not unique to  $\gamma$ -PNAs; this phenomenon has been well-documented in the literature for other classes of oligonucleotides.<sup>23–33</sup> However, for many of these systems helical induction is limited

(15) Dragulescu-Andrasi, A.; Rapireddy, S.; Frezza, B. M.; Gayathri, C.; Gil, R. R.; Ly, D. H. *J. Am. Chem. Soc.* **2006**, *128*, 10258–10267.

(16) Fechter, E. J.; Dervan, P. B. *J. Am. Chem. Soc.* **2003**, *125*, 8476–8485.

(17) Fechter, E. J.; Olenyuk, B.; Dervan, P. B. *Angew. Chem., Int. Ed.* **2004**, *43*, 3591–3594.

(18) Bentin, T.; Nielsen, P. E. *J. Am. Chem. Soc.* **2003**, *125*, 6378–6379.

(19) Rapireddy, S.; Ly, D. H., manuscript in preparation.

(20) Christensen, L.; Fitzpatrick, R.; Gildea, B.; Petersen, K. H.; Hansen, H. F.; Koch, T.; Egholm, M.; Buchardt, O.; Nielsen, P. E.; Coull, J.; Berg, R. H. *J. Pept. Sci.* **1995**, *1*, 175–183.

(21) Wittung, P.; Nielsen, P. E.; Buchardt, O.; Egholm, M.; Norden, B. *Nature* **1994**, *368*, 561–563.

(22) Egholm, M.; Buchardt, O.; Christensen, L.; Behrens, C.; Freier, S. M.; Driver, D. A.; Berg, R. H.; Kim, S. K.; Norden, B.; Nielsen, P. E. *Nature* **1993**, *365*, 566–568.

(23) Holcomb, D. N.; Tinoco, I. J. *Biopolymers* **1965**, *3*, 121–133.

(24) Leng, M.; Felsenfeld, G. *J. Mol. Biol.* **1966**, *15*, 455–466.

(25) Brahm, J.; Michelson, A. M.; Van Holde, K. E. *J. Mol. Biol.* **1966**, *15*, 467–488.

(26) Poland, D.; Vournakis, J. N.; Harold, A. *Biopolymers* **1966**, *4*, 223–235.

(27) Felsenfeld, G.; Miles, H. T. *Annu. Rev. Biochem.* **1967**, *36*, 407–448.

(28) Rawitscher, M. A.; Ross, P. D.; Sturtevant, J. M. *J. Am. Chem. Soc.* **1963**, *85*, 1915–1918.

(29) Stannard, B. S.; Felsenfeld, G. *Biopolymers* **1975**, *14*, 299–307.

(30) Saenger, W. In *Principles of Nucleic Acid Structure*, Springer Advanced Texts in Chemistry; Cantor, C. R., Ed.; Springer-Verlag: New York, 1984; pp 302–315.

(31) Vesnaver, G.; Breslauer, K. J. *Proc. Natl. Acad. Sci. U.S.A.* **1991**, *88*, 3569–3573.

(32) Isaksson, J.; Acharya, S.; Barman, J.; Cheruku, P.; Chattopadhyaya, J. *Biochemistry* **2004**, *43*, 15996–16010.

(33) Lebedev, A. V.; Wickstrom, E. *Perspect. Drug Discovery Des.* **1996**, *4*, 17–40.

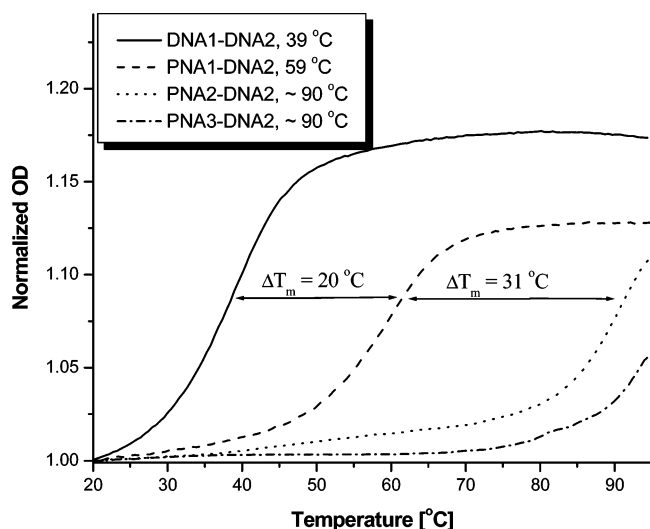


**Figure 2.** UV-melting profiles of PNA–DNA and DNA–DNA duplexes. The concentration of each strand was 5  $\mu\text{M}$ , prepared in 10 mM NaPi buffer (pH 7.4). Both the heating and the cooling runs were recorded, with both runs showing nearly identical profiles. The  $T_m$ s were determined by taking the first derivative of the melting curves.

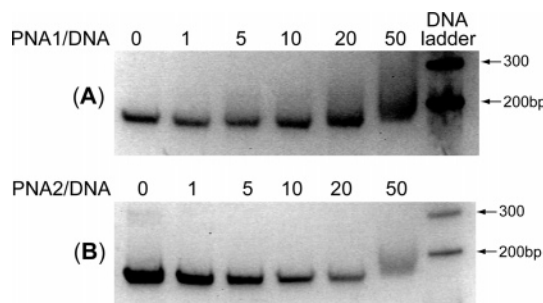


**Figure 3.** Gel-shift assay of (A) PNA1 and (B) PNA2 with 171-bp PCR fragment containing perfectly matched (PM) target. 0.4  $\mu\text{M}$  of DNA (duplex concentration) was incubated with various concentrations (0, 0.4, 2.0, 4.0, 8.0, and 20.0  $\mu\text{M}$ ) of PNA1 and PNA2 in 10 mM NaPi buffer at 37  $^\circ\text{C}$  for 1 h. The reaction mixtures were separated on non-denaturing polyacrylamide gel and stained with SYBR-Gold.

to purine-rich sequences. Helical induction in  $\gamma$ -PNAs, on the other hand, is not restricted to just purine-rich sequences, but is general to all four-nucleobase sequence composition.

**Thermal Stability.** Next, we compared the thermal stability of PNA2 and PNA3 to that of PNA1 following hybridization with the complementary DNA strand (DNA2) by UV-spectroscopic method. Samples containing stoichiometric amounts of PNA and DNA at 5  $\mu\text{M}$  strand concentration each were prepared in 10 mM NaPi buffer and annealed, and their UV-absorption at 260 nm was recorded as a function of temperature for both the heating and the cooling runs. Figure 2 shows the heating profiles of the various PNA–DNA hybrid duplexes, along with that of the corresponding DNA1–DNA2 duplex included for comparison. Our result shows a significant stabilization for the PNA2–DNA2 and PNA3–DNA2 duplexes, with  $T_m \approx 90$   $^\circ\text{C}$  for both as compared to 59 and 39  $^\circ\text{C}$  for PNA1–DNA2 and DNA1–DNA2, respectively, corresponding to a net gain in  $\Delta T_m$  of +31 and +51  $^\circ\text{C}$ . Inclusion of the acridine moiety had little effect on the thermal stability of the PNA2–DNA2 duplex. This level of stabilization is significant considering that no electrostatic interaction is involved and that the chiral  $\gamma$ -monomers can be prepared cheaply and in few steps in comparison with

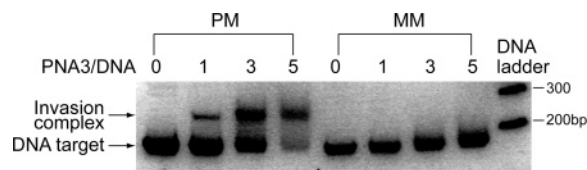
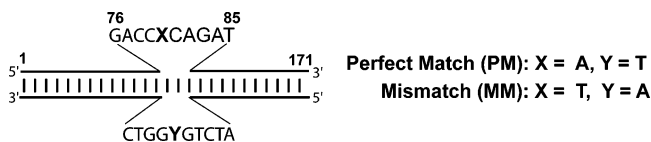


**Figure 4.** Gel-shift assay of PNA3 with 171-bp PCR fragment containing perfectly matched (PM) and single-based mismatched (MM) target. 0.4  $\mu\text{M}$  of each DNA duplex was incubated with various concentrations (0, 0.4, 1.2, and 2.0  $\mu\text{M}$ ) of PNA3 in 10 mM NaPi buffer at 37  $^\circ\text{C}$  for 1 h. The samples were separated and stained with SYBR-Gold under conditions identical to those described for PNA1 and PNA2 in Figure 3.

**Scheme 2.** An Illustration of the 171-bp Linear B-DNA Fragments Containing Perfectly Matched (PM) and Single-Base Mismatched (MM) Binding Sites Used in the Gel-Shift and Chemical Probing Assays



other chiral PNA monomers developed to date.<sup>34–38</sup> The only other nucleic acid mimic with comparable thermal stability is locked-nucleic acid (LNA),<sup>39–42</sup> which generally requires elaborate synthesis and is relatively expensive to prepare.

**DNA Strand Invasion.** To determine whether these oligonucleotides can strand invade B-DNA, we performed a gel-shift assay. A 171-bp linear PCR fragment containing a perfectly matched binding site (PM, Scheme 2) was incubated separately with various concentrations of PNA (PNA1) and  $\gamma$ -PNAs (PNA2 and PNA3) in 10 mM NaPi buffer at 37  $^\circ\text{C}$ . The complex mixtures were then separated on a non-denaturing polyacrylamide gel and stained with SYBR-Gold for visualization. Our result showed that with PNA/DNA ratios as high as 50:1 and incubation time as long as 16 h, no noticeable shift in the DNA bands was observed for either PNA1 (Figure 3A) or PNA2 (Figure 3B and Figure 3S (Supporting Information)), suggesting that either strand invasion did not take place or that the invasion complex was not sufficiently stable under the electrophoresis condition as reported for homopurine PNA.<sup>43</sup> Although smeared patterns were observed at high PNA/DNA ratios, this could be due to nonspecific binding. On the other hand, we observed a distinct, slow-moving band following incubation with PNA3 (Figure 4, under the heading PM). The intensity of the retarded band gradually increased with increasing PNA/DNA ratios and appears to be highly sequence-specific because no traces of the retarded band were observed when the target containing a single-base mismatch was used (Figure 4,

- (34) Beck, F.; Nielsen, P. E. In *Artificial DNA: Methods and Applications*; Khudyakov, Y. E., Fields, H. A., Eds.; CRC Press: Boca Raton, FL, 2003; pp 91–114.
- (35) Uhlmann, E.; Peyman, A.; Breipohl, G.; Will, D. W. *Angew. Chem., Int. Ed.* **1998**, *37*, 2796–2823.
- (36) Kumar, V. A.; Ganesh, K. N. *Acc. Chem. Res.* **2005**, *38*, 404–412.
- (37) Pokorski, J. K.; Witschi, M. A.; Purnell, B. L.; Appella, D. H. *J. Am. Chem. Soc.* **2004**, *126*, 15067–15073.
- (38) Corradini, R.; Sforza, S.; Tedeschi, T.; Marchelli, R. *Chirality* **2007**, *19*, 269–294.
- (39) Singh, S. K.; Koshkin, A. A.; Wengel, J.; Nielsen, P. *Chem. Commun.* **1998**, 455–456.
- (40) Obika, S.; Nanbu, D.; Hari, Y.; Andoh, J.-i.; Morio, K.-i.; Doi, T.; Imanishi, T. *Tetrahedron Lett.* **1998**, *39*, 5401–5404.
- (41) Varghese, O. P.; Barman, J.; Pathmasiri, W.; Plashkevych, O.; Honcharenko, D.; Chattopadhyaya, J. *J. Am. Chem. Soc.* **2006**, *128*, 15173–15187.
- (42) Srivastava, P.; Barman, J.; Pathmasiri, W.; Plashkevych, O.; Wenska, M.; Chattopadhyaya, J. *J. Am. Chem. Soc.* **2007**, *129*, 8362–8379.
- (43) Nielsen, P. E.; Christensen, L. *J. Am. Chem. Soc.* **1996**, *118*, 2287–2288.

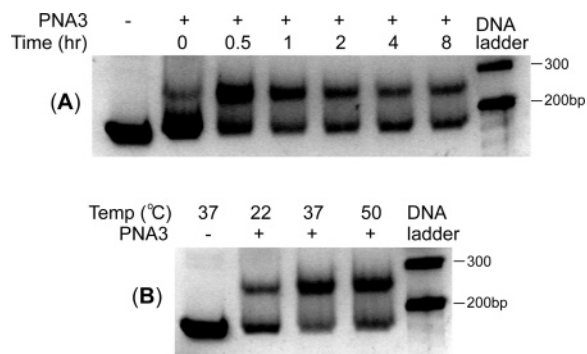


**Figure 5.** (A) Time-course and (B) temperature-dependent DNA strand invasion by PNA3. Samples containing  $0.4 \mu\text{M}$  of perfectly matched DNA target and  $2.0 \mu\text{M}$  of PNA3 were prepared in 10 mM NaPi buffer (pH 7.4) and incubated (A) at  $37 \text{ }^\circ\text{C}$  for various time-periods and (B) for 1 h at various temperatures. A gradual loss of DNA over time in (A) could be due to nonspecific adsorption of DNA onto the wall of the sample tubes as the result of prolonged incubation.

under the heading MM). Time-course study showed that formation of the complex reached saturation within 30 min of incubation (Figure 5A); longer incubation times did not result in further increase in the quantity of this complex. Temperature-dependent study further showed that formation of this complex occurred even at room temperature, but was more efficient at higher temperatures ( $37$  and  $50 \text{ }^\circ\text{C}$ ) as reflected in the intensity of the retarded bands (Figure 5B). There is no difference in the intensity of the shifted band whether the incubation was made at  $37$  or at  $50 \text{ }^\circ\text{C}$ , indicating that equilibrium is reached at both temperatures in less than one hour, consistent with the time-course results.

**DNA Strand Displacement.** To further confirm that PNA3 binding is sequence-specific and occurred through strand invasion, we performed a chemical probing experiment. In this case, DEPC (diethyl pyrocarbonate) was used because it is known to react selectively with adenines and to a lesser extent with guanines of a perturbed or single-stranded DNA region,<sup>44,45</sup> which would occur upon strand invasion by PNA3, that can be revealed through strand cleavage following piperidine treatment. As expected, DEPC-treatment of the invading complex, with the 3'-end of the homologous strand labeled with P-32, revealed selective cleavage of the homologous strand at the adenine and to a lesser extent at the guanine sites in a region where PNA3 was expected to bind, Figure 6. Strand displacement, in this case, appears to be highly sequence-specific because no strand cleavage pattern was observed for the homologous strand containing a single-base mismatched target (MM, Scheme 2). This result is consistent with the gel-shift assay, showing that PNA3 binding is sequence-specific and occurs through strand invasion via Watson–Crick base-pairing.

## Conclusion

In summary, we have shown that conformationally preorganized  $\gamma$ -PNA containing acridine moiety at the C-terminus can strand-invade mixed-sequence B-DNA in a sequence-specific manner through direct Watson–Crick base-pairing. The invasion process is just as efficient at physiological as at elevated temperatures and appears to be relatively fast, reaching equilibrium within 30 min of incubation. Although the role of

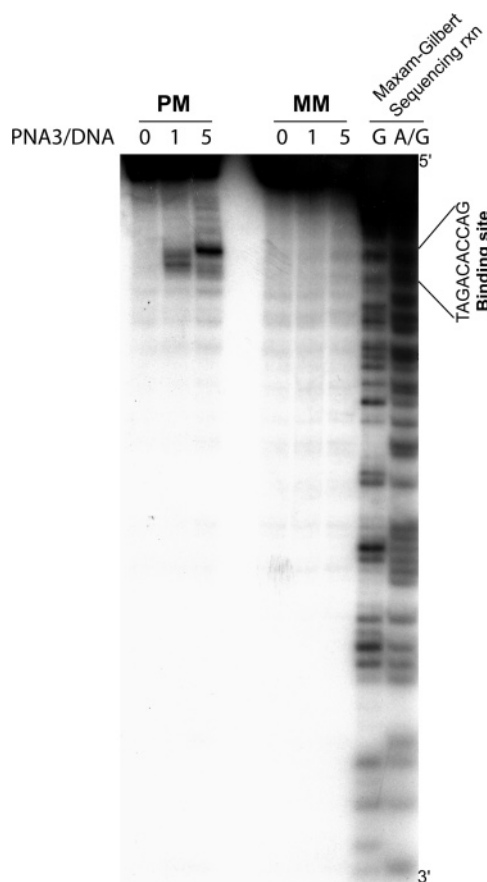


**Figure 6.** Results of DEPC-treatment following incubation of 171-bp PCR fragments containing perfectly matched (PM) and single-base mismatched (MM) target with PNA3. The homologous strand was 3'-labeled with P-32. 10 000 cpm of the labeled and  $0.4 \mu\text{M}$  of the cold (unlabeled) DNA were incubated with 0, 0.4, and  $2.0 \mu\text{M}$  of PNA3 in 10 mM NaPi buffer at  $37 \text{ }^\circ\text{C}$  for 1 h, followed by DEPC-treatment. The samples were separated on denaturing polyacrylamide gel, and the cleavage patterns were visualized by autoradiography.

acridine in assisting PNA3 invasion of B-DNA is not precisely known, it is likely to confer its effect through intercalation, presumably at the melted region (Y-junction) of the DNA duplex. Such intercalation would help minimize PNA–DNA end-fraying, thereby providing the necessary binding free energy for PNA3 to invade B-DNA. A similar effect of acridine in promoting strand invasion by homopyridine PNA was reported by Bentin and Nielsen.<sup>18</sup> The ability to target B-DNA through direct Watson–Crick base-pairing is important because, in addition to its simplicity, this strategy has the potential to overcome many of the structural and/or conformational mismatched issues presently facing other classes of molecules designed to bind in the minor-<sup>46,47</sup> and major-grooves<sup>48,49</sup> of B-DNA. However, for  $\gamma$ -PNAs as well as for many other classes of chiral nucleic acid mimics,<sup>50–54</sup> maintaining stereoregularity

(44) Scholten, P. M.; Nordheim, A. *Nucleic Acids Res.* **1986**, *14*, 3981–3993.

(45) Furlong, J. C.; Lilley, D. M. J. *Nucleic Acids Res.* **1986**, *14*, 3995–4007.

(46) Kelly, J. J.; Baird, E. E.; Dervan, P. B. *Proc. Natl. Acad. Sci. U.S.A.* **1996**, *93*, 6981–6985.

(47) Kielkopf, C. L.; Baird, E. E.; Dervan, P. B.; Rees, D. C. *Nat. Struct. Biol.* **1998**, *5*, 104–109.

(48) Gowers, D. M.; Fox, K. R. *Nucleic Acids Res.* **1999**, *27*, 1569–1577.

(49) Jantz, D.; Amann, B. T.; Gatto, G. J.; Berg, J. M. *Chem. Rev.* **2004**, *104*, 789–800.

(50) Demesmaeker, A. D.; Altmann, K. H.; Waldner, A.; Wendeborn, S. *Curr. Opin. Struct. Biol.* **1995**, *5*, 343–355.

(51) Vyazovkina, E. V.; Savchenko, E. V.; Lokhov, S. G.; Engels, J. W.; Wickstrom, E.; Lebedev, A. V. *Nucleic Acids Res.* **1994**, *22*, 2404–2409.

(52) Kean, J. M.; Cushman, C. D.; Kang, H.; Leonard, T. E.; Miller, P. S. *Nucleic Acids Res.* **1994**, *22*, 4497–4503.

and optical purity is essential to achieving optimal hybridization properties and, in the case of  $\gamma$ -PNAs, DNA invasion capabilities. It should also be pointed out that, like other PNA binding modes,<sup>4</sup> DNA strand invasion by  $\gamma$ -PNA is most effective at relatively low ionic strength. Additional work will be required to further improve the binding energetics of  $\gamma$ -PNA so that DNA strand invasion could take place at physiologically relevant ionic strength, an essential requirement for in vivo applications.

(53) Boczkowska, M.; Guga, P.; Stec, W. J. *Biochemistry* **2002**, *41*, 12483–12487.

(54) Lesnikowski, Z. J. *Bioorg. Chem.* **1993**, *21*, 127–155.

**Acknowledgment.** Funding was provided in part by the National Institutes of Health to D.H.L. (GM076251-01).

**Supporting Information Available:** UV-melting profiles of individual PNA and  $\gamma$ -PNA strands (Figure 1S), UV-melting profiles of PNA3–DNA duplexes containing perfectly match and single-base mismatch (Figure 2S), gel-shift assay of PNA2 with perfectly matched DNA after 16 h incubation (Figure 3S), and other experimental protocols. This material is available free of charge via the Internet at <http://pubs.acs.org>.

JA074886J